



The effect of nutrient limitation on bacterial wax ester production

Laura K. Martin, Wei E. Huang, Ian P. Thompson^{*}

Department of Engineering Science, University of Oxford, Parks Road, Oxford OX1 3PJ, United Kingdom

ARTICLE INFO

Keywords:

Wax ester
Lipid accumulation
Nutrient limitation
Nitrogen
Phosphate
Acinetobacter baylyi ADP1
Microbiology
Biotechnology
Bioproduction

ABSTRACT

Nutrient limitation is widely employed to alter the behaviour of micro-organisms. Here, the impact of nitrogen and, for the first time, phosphate limitation is investigated on the production of bacterial storage lipids; specifically wax esters, a class of storage lipids of industrial interest, by the bacterium *Acinetobacter baylyi* ADP1 grown on the low-cost substrate acetate. Studies determined the absolute and temporal effects of nutrient limitation and identified a maximum wax titre of 132 mg/L and content of 17 % of biomass. A 4-fold increase in wax production was achievable by manipulating carbon: phosphate ratio. Multivariable analysis identified a novel interaction effect between carbon: nitrogen and carbon: phosphate ratios on wax production. Extreme phosphate starvation shifted the dominant lipid class from wax esters to triacylglycerols, the first report of the potential of phosphate limitation to alter the type of lipid generated. These findings offer valuable insights for future microbial bioproduction studies.

1. Introduction

Nutrient limitations are among the most common stresses experienced by micro-organisms and are known to have significant and varied effects on growth and physiology. When faced with essential nutrient depletion, growth is typically limited, and carbon and energy fluxes are redirected towards increasing the bioavailability of the desired nutrient (Gupta and Laxman, 2021; Liu et al., 2016; Zhang et al., 2016). Whether by upregulating proteins and pathways for extracellular scavenging or degrading non-essential intracellular metabolites (Peterson et al., 2005), the need to source a scarce element significantly alters the metabolism of a micro-organism (Ikaran et al., 2015; Wang et al., 2018). However, assuming that the period of limitation will be brief, in some microbes nutrient starvation also activates additional metabolic pathways to monopolise resources for the future.

Carbon storage molecules are a common example of such microbial ‘future-proofing’. These molecules, typically in the form of carbon-dense lipids, are accumulated intracellularly as an alternative to growth when essential nutrients are limited, but carbon is plentiful. One specific lipid class of interest is wax esters (WEs). These long chain esters are hydrophobic and chemically inert, making them highly desirable for a wide range of applications, from cosmetics and food additives to industrial lubricants (Bart et al., 2013; Santala et al., 2011a). They comprise the major component of many highly desirable biologically derived waxes, including jojoba and spermaceti oils, widespread usage

of which is restricted by expensive and unethical sourcing, respectively. An alternative source of WEs is therefore of great industrial interest.

Although a range of microbial species are capable of accumulating high concentrations of storage lipids (Lennen and Pfeleger, 2013; Martin et al., 2021), these are typically a mixture of triacylglycerols (TAGs), diacylglycerols (DAGs) and fatty acids. WEs are less prevalent due to the scarcity of endogenous long chain fatty acid reductase enzymes in micro-organisms, which are essential to generate the fatty alcohol required for esterification (Cronan and Thomas, 2009). Such enzymes are, however, present in the bacterial species *Acinetobacter baylyi* ADP1, which is widely known for its ability to accumulate WEs (Ishige et al., 2003; Santala and Santala, 2021). While storage lipid composition in this species has been shown to be substrate-dependent (Salcedo-Vite et al., 2019), WEs always comprise the major component. In addition, ADP1 is well characterised, with a fully sequenced genome, and is naturally competent for transformation of DNA (Santala and Santala, 2021). While this study focuses on the effects of nutrient limitation in the wild type (WT) bacteria, findings here can be easily translated to engineered and mutant strains, potentially further improving the yields and titres achieved.

Previously, most researchers have focused on nitrogen as the limiting nutrient, which has been shown to increase lipid accumulation in a wide range of bacteria (Manilla-Pérez et al., 2011), yeast (Pomraning et al., 2016), algae (Ikaran et al., 2015) and microalgae (Wang et al., 2019), although the optimal degree of N-limitation is rarely determined.

^{*} Corresponding author.

E-mail address: ian.thompson@eng.ox.ac.uk (I.P. Thompson).

<https://doi.org/10.1016/j.biteb.2023.101423>

Received 6 January 2023; Received in revised form 30 March 2023; Accepted 31 March 2023

Available online 5 April 2023

2589-014X/© 2023 The Authors. Published by Elsevier Ltd. This is an open access article under the CC BY license (<http://creativecommons.org/licenses/by/4.0/>).

However, many economical and sustainable substrates are mixed waste streams inherently high in nitrogen (Luo et al., 2020). For this reason, alternative nutrient limitation strategies to induce lipid accumulation are of interest. Fortunately, starvation of phosphate, another essential nutrient, has also been found to result in lipid production in yeast (Huang et al., 2018; Wang et al., 2018), algae (Shrestha et al., 2020) and micro-algae (Yang et al., 2018a), although its effect on bacterial storage lipid accumulation has not been investigated.

The effect of combined limitation of both nitrogen and phosphate, and any interaction between these factors, has also been largely ignored in the literature; where tested, results have been inconsistent. In microalgae, Yang et al found excess phosphate with N limitation gave the highest lipid titres and content (% CDW), followed by P and N limitation, then N-limitation with sufficient P, with sufficient N and P resulting in the least lipid production (Yang et al., 2018b). Conversely, Wierzychowska et al took two different approaches to lipid accumulation in yeast; initially detecting no significant effect of N on lipid content, then observing the optimal combination was simultaneous N and P limitation (Wierzychowska et al., 2021). This limited and conflicting data on such key growth parameters highlights the need for further investigation in this area.

As well as macronutrients, micronutrients are also known to affect both microbial growth and lipid accumulation. Divalent cations magnesium (Mg^{2+}) and calcium (Ca^{2+}) are of particular importance to cell function, with the former used for metabolic enzymes, nucleic acid stabilisation and DNA replication (Walker, 1994), and the latter in structure, transport and gene expression (Dominguez, 2004). Limitation of both has been demonstrated to reduce bacterial growth (Chen et al., 2019; Lusk et al., 1968). Furthermore, increasing the concentration of both ions has also been demonstrated to improve lipid production in freshwater and marine microalgae (Huang et al., 2014; Singh et al., 2016). Increasing the concentration of potassium (K^+), the main bacterial cation, used as a messenger and for maintaining pH and membrane potential (Deshpande et al., 2013), has also been shown to increase lipid accumulation, particularly of fatty acids, in microalgae (Janchot et al., 2019). However, despite the demonstrated benefits on a range of other micro-organisms for lipid accumulation, there has been little exploration of the effects of these key micronutrients on bacterial lipid production.

Substrate choice is vital to the feasibility of microbial biosynthesis processes. Currently, glucose and other sugars dominate studies of microbial lipid synthesis (Kannisto et al., 2014; Luo et al., 2020; Martin et al., 2021; Rottig et al., 2016; Round et al., 2019), and, with WE titres of up to 0.58 g/L achieved from growth on glucose employing WT ADP1 (Luo et al., 2020), the attractiveness of such feedstocks is evident. Unfortunately, sugars are expensive and their production requires arable land to grow high-sugar fuel crops, igniting land-use conflicts with food production, housing and natural ecosystems (Mohr and Raman, 2013). With this in mind, the utilisation of waste-stream derived substrates is becoming increasingly attractive. Acetate (or acetic acid) can be produced from a wide range of waste streams. Anaerobic digestion, commonly used to degrade mixed biological waste into biogas for fuel, can be tuned to produce high yields of acetic acid, as well as other volatile fatty acids also suitable for fermentation (Patel et al., 2021). Alternatively, microbial electrosynthesis can fix CO_2 from the atmosphere into platform chemicals, such as acetate (Kong et al., 2020). Moreover, several researchers have demonstrated the potential of acetate as a substrate for WE production in ADP1, which is able to utilise the substrate either in a co-feeding system with another, higher energy, feedstock (Santala et al., 2021) or as a sole carbon and energy source (Lehtinen et al., 2017; Santala et al., 2018).

In this study, the effect of several micro and macro nutrients on the production of wax esters from acetate as a sole carbon source by ADP1 was explored. Thorough single factor studies were performed by limiting the macro-nutrients nitrogen and phosphate, with a range of conditions explored to identify any trends or significant behavioural changes over

the experimental space and identify a narrower range of interest. The temporal variation of wax production was also monitored to explore how production and consumption of WEs varied under different conditions and to accurately compare maximum wax production under different conditions, accounting for differences in growth behaviour. Total wax titre, intracellular concentration and percentage yield of waxes were all calculated to provide a comprehensive account of the different benefits of wax production under different conditions. Binary studies of the effects of micronutrients calcium, potassium, magnesium, and a common trace elements mix were also conducted. From this initial data, an optimised, multi-factor experiment was conducted, to identify any interaction effects of nitrogen and phosphate limitation under the most optimal micronutrient conditions.

2. Materials and methods

2.1. Chemicals

All chemicals were sourced from SigmaAldrich (Merck).

2.2. Media

The standard mineral medium contained 4.18 g/L MOPS buffer and 0.1 g/L $MgSO_4 \cdot 7H_2O$, adjusted to pH 6.8 with NaOH and sterilised by autoclave. Concentrated solutions of 300 g/L sodium acetate, 100 g/L NH_4Cl , 200 g/L KH_2PO_4 , 85 g/L K_2SO_4 , 1000 g/L $CaCl_2 \cdot 2H_2O$, 1000 \times solution Bauchop & Elsden (TE) (Bauchop and Elsden, 1960) and saturated $FeSO_4$ were prepared and sterilised separately and added to the media immediately prior to starting the experiment. The standard media recipe contained 10 μ L/L of $CaCl_2$ and $FeSO_4$ stocks, 1 mL/L of TE solution and 150 mM (or 41 mL/L) of sodium acetate stock. In each condition, pH was readjusted aseptically to 6.8 before inoculation.

2.3. Culture conditions

Bacterial stocks were stored at $-80^\circ C$ in 20 % glycerol/water. Stocks were plated on LB agar and incubated at $30^\circ C$ for 24 h, with a single colony transferred in LB liquid media and grown until mid-exponential phase. Bacteria were pre-cultured twice in conical flasks in mineral medium with acetate and excess N and PO_4 and transferred during mid-exponential phase. Immediately prior to starting each experiment, pre-cultures were spun down at 6000 g for 6 min, resuspended in MOPS buffer and flasks were inoculated at an initial OD of 0.1. Experiments were performed in 200 mL cultures in 1 L conical flasks, in triplicate. All liquid cultures, and pre-cultures, were cultivated at $30^\circ C$ and 150 rpm.

2.4. Nitrogen, phosphate and micronutrient limitation studies

NH_4Cl and KH_2PO_4 stocks were added as required to achieve the desired C:N or C: PO_4 molar ratios for each experiment. K_2SO_4 was used to maintain a constant K^+ concentration of 15 mM under all conditions. Under N limitation, excess PO_4 at C: PO_4 of 20:1 was used, while under phosphate limitation excess N at C:N of 10:1 was used. Nitrogen and phosphate concentrations were quantified experimentally using spectrophotometric kit-based assays (Hach Lange: LCK 303 for ammonia and LCK 349/LCK 350 for phosphate, results in supplementary information). Where micronutrients were varied, the concentration of $CaCl_2$, $MgSO_4$, K_2SO_4 or TE solutions were varied accordingly.

2.5. Growth curves and cell dry weight measurements

Growth was measured by absorbance at 600 nm with UV-1800 UV/Vis spectrophotometer (Shimadzu, Kyoto, Japan). For cell dry weight and lipid extractions, 15–40 mL of cultures (depending on OD) were extracted and centrifuged for 8 min at 10,000 g. Cell pellets were resuspended in 1.5 mL of DI water, transferred to an Eppendorf tube and

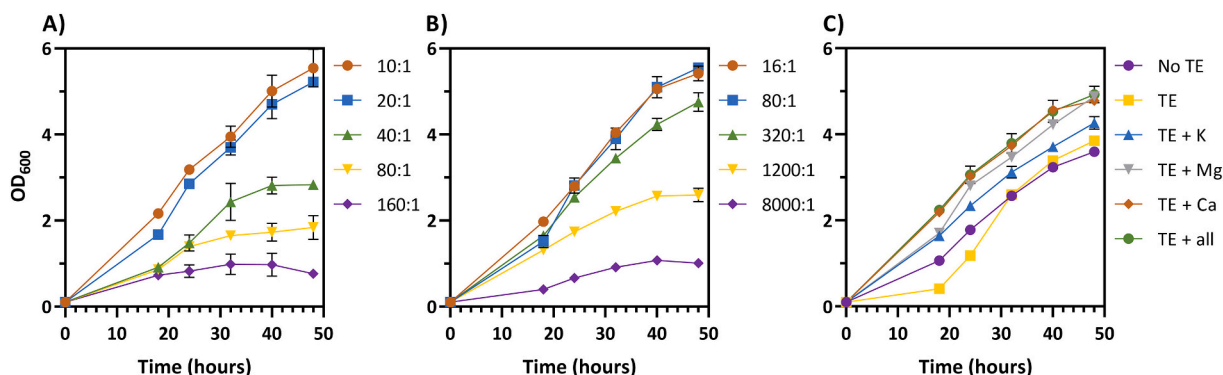


Fig. 1. Growth curves for ADP1 grown on 150 mM acetate under A) different C:N ratios, B) different C:PO₄ ratios and C) under different micronutrient conditions. Individual points are means of biological replicates ($n = 3$), error bars are standard deviations.

centrifuged for 5 min at 13,000 g. Washed cell pellets were lyophilised overnight and the biomass determined gravimetrically.

2.6. Lipid extraction and quantification

For NMR quantification, lipids were extracted following an adapted Bligh and Dyer method (Santala et al., 2011b). Each cell pellet was resuspended in 2 mL of PBS, then 2.5 mL chloroform and 5 mL of methanol were added and the mixture shaken for approx. 5 h at 150 rpm. 2.5 mL of methanol, 2.5 mL PBS and 2.5 mL of chloroform were then added, the sample mixed again and stored overnight at +4 °C. The suspension was centrifuged at 10,000 g for 8 min, and the lower organic phase was transferred to a pre-weighed glass vial to evaporate. The aqueous phase was extracted again by addition of 5 mL of chloroform, mixed and incubated overnight at +4 °C, then centrifuged and separated as before.

NMR analysis was performed using Bruker Avance III spectrometer (700 MHz) with a TCI cryoprobe (Bruker, MA, US). Lipid samples were dissolved in 600 μ L of chloroform- d_3 and 1 H spectra recorded at ambient temperature. Spectra were processed and analysed using MestreNova 14.1.1. with an artificial reference peak at $\delta -1$ ppm, corresponding to a single hydrogen atom with concentration of 10 mM. Global Spectrum Deconvolution was used to accurately isolate and integrate the triplet peak at $\delta 4.05$ ppm, corresponding to the 2 α -alkoxy methylene protons from the alcohol component of WEs. From this the WE concentration was determined and used to calculate the mass of WEs produced, assuming an average Mw for WEs of 506 g/mol (Lehtinen et al., 2018). Where present, TAGs were quantified from the same NMR spectra from the doublet of doublet peak at $\delta 4.29$ ppm (Nieva-Echevarría et al., 2014), corresponding to 2 of the ROCH₂-CH(OR')-CH₂OR" protons. An average Mw of 847.4 g/mol was used to calculate mas of TAGs, assuming an approximately equal likelihood of C16 or C18 fatty acids esterified to each glycerol alcohol, as these are the most prevalent fatty acids in acetate-grown ADP1, and an average of 1 unsaturated C=C bond per TAG (Salcedo-Vite et al., 2019).

2.7. Acetate consumption and C-Conversion

Remaining acetate content at each time point was measured from the supernatant of the extracted cells for CDW and WE quantification using gas chromatography-flame ionisation detection (GC-FID) (Shimadzu GC-2010) with a 30 m \times 0.25 mm \times 0.25 μ m fused-silica capillary column (ZB-FFAP). The temperatures of the detector and injector were set at 350 °C and 250 °C, respectively. The oven temperatures were set at 100 °C for 2 min and then increased at a rate of 16 °C/min. Calibration was performed with standards of sodium acetate at concentrations from 0.31 to 20.00 g/L. All samples and standards (450 μ L) were acidified with 10 % v/v of formic acid (50 μ L) prior to analysis. C-conversion

efficiency was calculated from the total acetate consumption for each sample.

2.8. Multivariable experiment

Based on the optimal C:N and C:PO₄ ranges and the optimal micronutrient condition identified, a multivariable experiment was conducted. A 2-factor, central composite designed experiment was constructed and analysed using OriginPro 2022b 'Design of Experiments' application (OriginLab, Northampton, MA, United States). Experimental C:N and C:PO₄ ratios were quantified and confirmed to agree with intended values. Each condition was replicated in biological duplicate, with 4 replicates of the centre point, and data was blocked by axial/equatorial group and replicate. Samples for WE analysis were taken every 8 h from 24 to 56 h. The maximum value, for titre and content, was taken from each replicate individually, regardless of time point, and maximum average was calculated from this. Data analysis was performed in the application, resulting in a fitted response surface for both titre and content of WE, TAG and combined lipids.

2.9. Statistical analysis

All results were analysed for statistical significance in GraphPad Prism (GraphPad, San Diego, CA, United States). For single variable experiments, time-dependent data across all conditions was analysed by a mixed-effects model to determine the effect of Time, condition and the interactions between the two. The maximum of each metric was identified for each condition over the whole time-course, and each set of maxima were analysed by One-Way ANOVA, with multiple pairwise comparisons. The Šidák correction was applied to control the false positive rate, and the Brown-Forsythe test was performed to confirm that group variances were not significantly different (and hence that the data was suitable for ANOVA).

For the multivariable experiment, statistical analysis was performed in OriginPro 2022b. The significance of each variable, and their interaction, on the model was analysed by a *t*-test on the coded co-efficients and analysis of variance (ANOVA) on the significance of the model components.

Asterisks indicate significance at different levels as follows: * = 0.05, ** = 0.01, *** = 0.001 and **** = 0.0001.

3. Results and discussion

3.1. Nitrogen limitation

The effect of nitrogen limitation was explored by varying the C:N molar ratio at a constant carbon concentration over the range of 10:1 (found by preliminary experiments to be in excess and produce

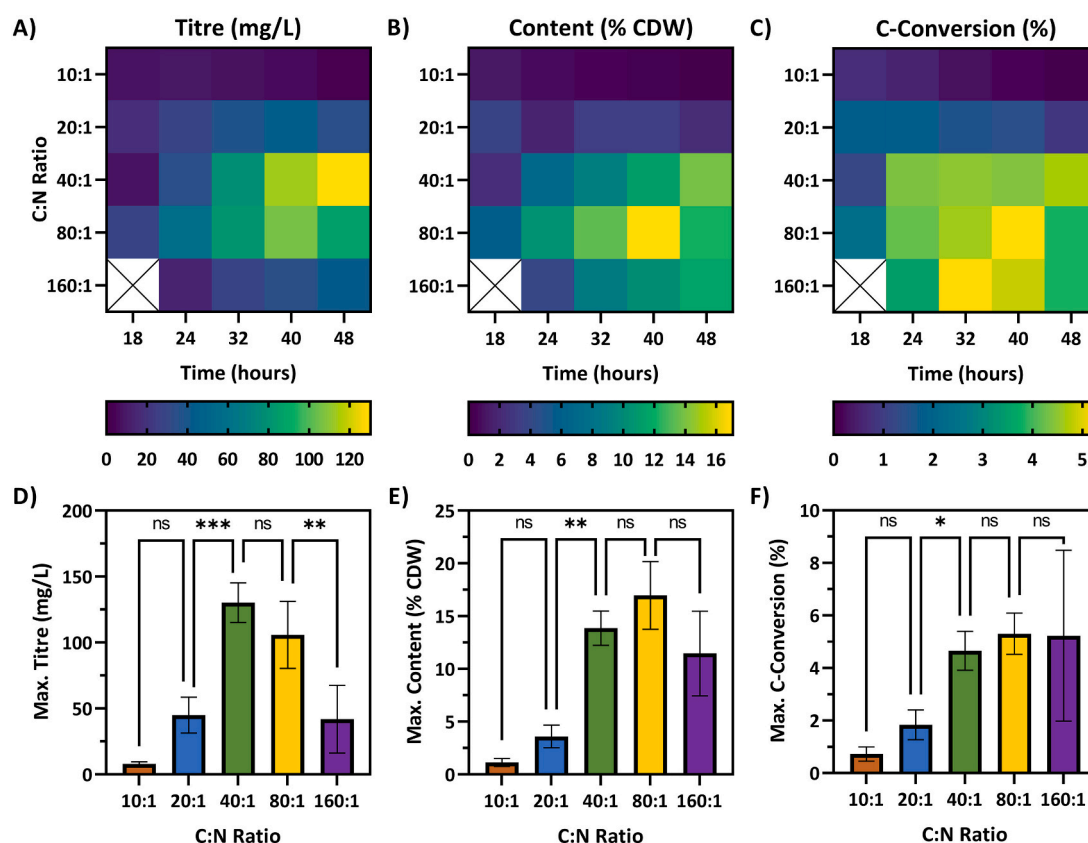


Fig. 2. Heat maps showing **A)** WE titre (mg/L), **B)** WE content per biomass (% CDW) and **C)** Carbon conversion efficiency from acetate to WEs (%), over time under different C:N ratios from 10:1 to 160:1. Data shows means of 3 biological replications (except for 10:1, where $n = 2$), values from blue (low) to yellow (high). Maximum achieved **D)** WE titre (mg/L), **E)** WE content per biomass (% CDW) and **F)** Carbon conversion efficiency to WEs for each condition. Data shows means and error bars represent standard deviation ($n = 3$ for all but 10:1, where $n = 2$). Pairwise statistical significance testing performed by ANOVA between sequential conditions, ns ≥ 0.05 , * = 0.05, ** = 0.01, *** = 0.001, **** = 0.0001. (For interpretation of the references to colour in this figure legend, the reader is referred to the web version of this article.)

maximum growth) to 160:1, similar to values trialed in literature which reported substantial lipid accumulation (Manilla-Pérez et al., 2011). As expected, growth was severely impaired by nitrogen limitation at C:N 40:1 and above, and became more variable with greater nitrogen depletion (Fig. 1A). However, despite nitrogen concentration halving sequentially between 20:1, 40:1, 80:1 and 160:1, in each case the maximal growth of the lower-nitrogen culture exceeded half that of the one above it, in agreement with previous literature (Manilla-Pérez et al., 2011). Cultures at 10:1 and 20:1 C:N consumed almost all the acetate present in 48 h, while in all other conditions acetate consumption plateaued and significant quantities of acetate remained even after 48 h. Cultures containing less nitrogen consumed less acetate, in agreement with the reduced growth, though acetate consumption was still observed after growth had plateaued.

Fig. 2 shows WE titre, content and carbon conversion efficiency over 48 h and statistical comparisons of the maximum achieved for each C:N condition. A final time point was taken at 64 h, but in all cases OD, CDW, wax titre and content had decreased, indicating cells had entered death phase, and hence this was not included. Wax titre and content per cell in 10:1 samples was very low across all time points, with a maximum titre of 8 ± 2 mg/L after 24 h, or content of 1.1 ± 0.4 % CDW after 18 h, both of which decreased over time. At 20:1, both content and titre were higher across the whole time-course, with a comparable trend to 10:1, but with maxima of 40 ± 10 mg/L and 4 ± 1 % CDW, after 40 and 18 h respectively.

WE generation was massively increased at 40:1 and 80:1 C:N, and increased with time, reaching maximum titres and contents of 130 ± 10 mg/L and 14 ± 2 % for 40:1 after 48 h and 110 ± 30 and 17 ± 3 % for

80:1 after 40 h, respectively. By 160:1 WE content reduced slightly and became more variable, at 11 ± 4 %, while titre was hindered by poor growth, with a maximum of 40 ± 30 mg/L. The extreme uncertainty in titre was a consequence of substantial variability in both growth and WE production due to extreme N starvation. Maximum carbon conversion efficiency increased with C:N ratio, most notably between 20:1 and 40:1, to a maximum of 5.3 ± 0.8 % at 80:1 after 40 h. At 160:1 carbon conversion efficiency remained high, however the maximum was much earlier (24 h) and showed more variability (5 ± 3 %).

A mixed effects statistical model identified C:N ratio had a significant effect on WE titre ($p < 0.01$), content ($p < 0.001$) and conversion efficiency ($p < 0.05$). By the same analysis, time had a significant impact on titre ($p < 0.01$), content ($p < 0.01$) and conversion efficiency ($p < 0.05$), respectively. This is consistent with 40:1, 80:1 and 160:1 showing increasing titre and content with time, while 10:1 and 20:1 showed little change. Conversely, at 10:1 and 20:1 conversion efficiency decreased with time, while at 40:1–160:1 it increased initially, but the effect then varied by condition.

The maximum of each metric was identified for each C:N ratio over the whole time-course. Pairwise comparisons were performed by One-Way ANOVA between the maxima for sequential C:N ratios, as shown in Fig. 2D, E and F. No significant difference in titre or content was detected between 10:1 and 20:1, but at 40:1 both were higher ($p < 0.001$ and $p < 0.01$, respectively). From 40:1 to 80:1 there was again no significant difference in either metric, but titre showed a significant decrease from 80:1 to 160:1 ($p < 0.05$) although the change in content was not significant due to the high variation. For C-conversion efficiency (Fig. 2F), Welch's ANOVA was performed, which removes the

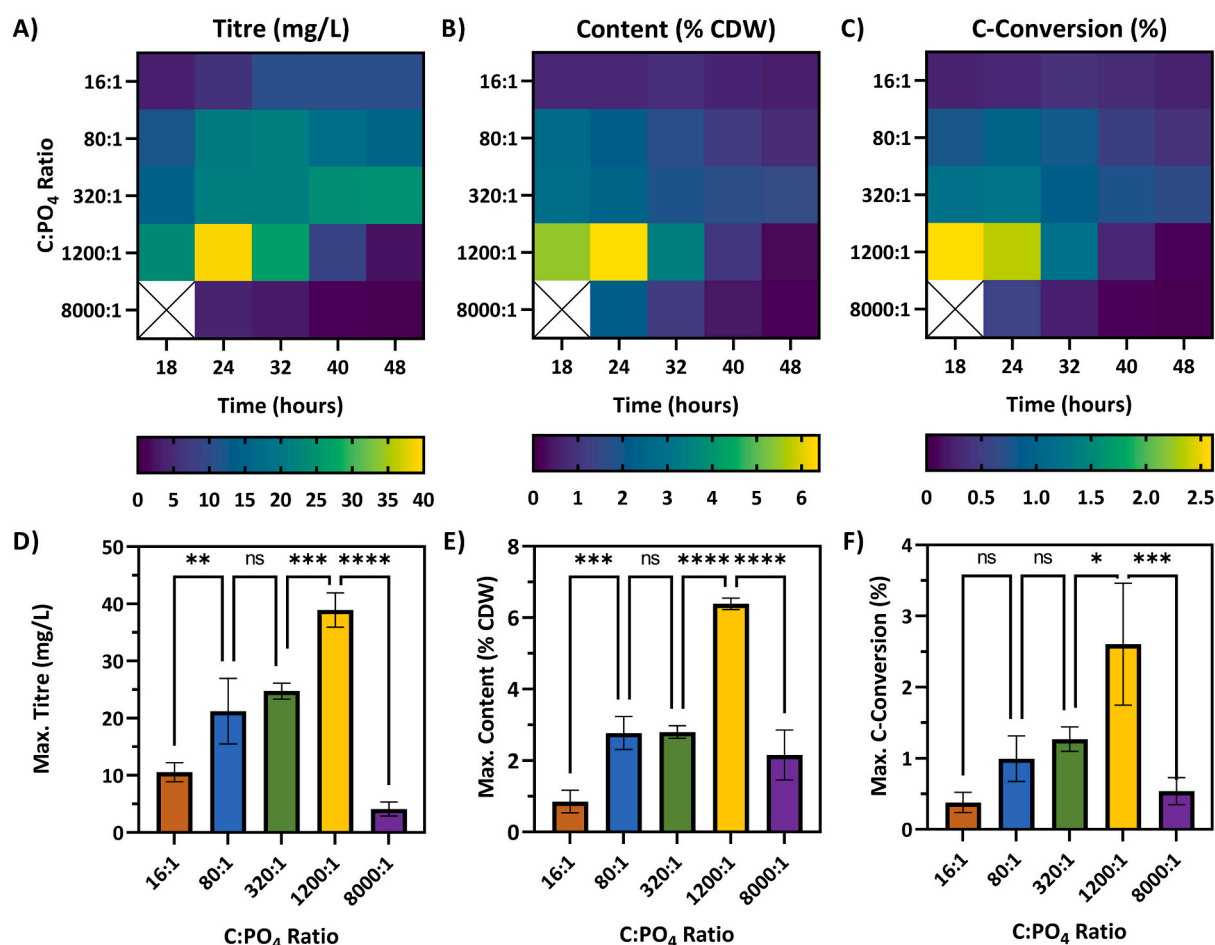


Fig. 3. Heat maps showing A) WE titre (mg/L), B) WE content per biomass (% CDW) and C) Carbon conversion efficiency from acetate to WEs, over time under different C:PO₄ ratios from 16:1 to 8000:1. Data shows means of 3 biological replicates, values from blue (low) to yellow (high). Maximum achieved D) WE titre (mg/L), E) WE content per biomass (% CDW) and F) Carbon conversion efficiency to WEs for each condition. Data shows means and error bars represent standard deviation ($n = 3$). Pairwise statistical significance testing performed by ANOVA between sequential conditions, ns ≥ 0.05 , * = 0.05, ** = 0.01, *** = 0.001, **** = 0.0001. (For interpretation of the references to colour in this figure legend, the reader is referred to the web version of this article.)

assumption of equal variance between samples given the large relative variation in 160:1. In this case, the overall effect of C:N on C-conversion efficiency was significant ($p < 0.01$), and sequential comparisons showed a significant increase in efficiency between 20:1 and 40:1 ($p < 0.05$).

While the effect of nitrogen limitation on accumulation of WEs is well documented (Luo et al., 2020; Shrestha et al., 2020), there have been relatively few systematic studies to identify the degree of nitrogen limitation which affords optimal results, especially in bacteria. The trade-off between growth limitation and lipid accumulation is crucial, as demonstrated here; if limitation is too extreme (C:N 160:1) then, regardless of the efficiency, poor growth limits absolute WE concentration. A moderate limitation (in the range of 40:1–80:1) is therefore more effective for high WE titres.

It is often assumed that greater N limitation yields a higher WE content per cell, even if growth is poor. Many two-stage WE production studies, in which cells are initially grown in media replete in nutrients and then starved of nitrogen to induce lipid accumulation, therefore employ minimal nitrogen in the second stage (Manilla-Pérez et al., 2011; Poontawee, 2020; Salcedo-Vite et al., 2019). However, maximum WE content per cell was actually achieved in the range of 40:1–160:1 C:N, indicating that this assumption may be false. Furthermore, there was no significant loss in conversion efficiency by employing moderate rather than extreme nitrogen limitation, suggesting more moderate limitations could be more effective across all metrics and for multiple process

designs.

As well as indicating the optimal C:N range for further exploration (see Section 3.4), these findings are of particular interest for the valorisation of waste streams as industrial bacterial feedstocks. Most waste streams contain significant amounts of nitrogen due to relatively high protein contents (Luo et al., 2020), and concentration typically varies between batches due to changes in composition. While both concentration and variability can be reduced through industrial treatments, strict requirements of very low, or specific, N concentrations are difficult and costly to achieve. The identification of a broad range of values within which production is high and consistent therefore makes utilisation of such feedstocks more feasible.

3.2. Phosphate limitation

ADP1 was also grown at a range of C:PO₄ molar ratios with excess nitrogen (C:N of 10:1). Based on previous literature (Wu et al., 2010), a range of 16:1 to 8000:1 was initially explored, with results shown in Fig. 3. The lowest ratio of these conditions (16:1) represented an excess of phosphate, while at ratios $> 320:1$ phosphate starvation occurred, and growth was limited (Fig. 1B). As in the nitrogen limitation study, excess phosphate resulted in consistently low WE titres and contents per cell over the entire period, with a maximum of just 11 ± 2 mg/L and 0.9 ± 0.3 % CDW. Ratios of 80:1 and 320:1 both initially showed slight WE accumulation, but at 80:1 WEs were subsequently depleted, while at

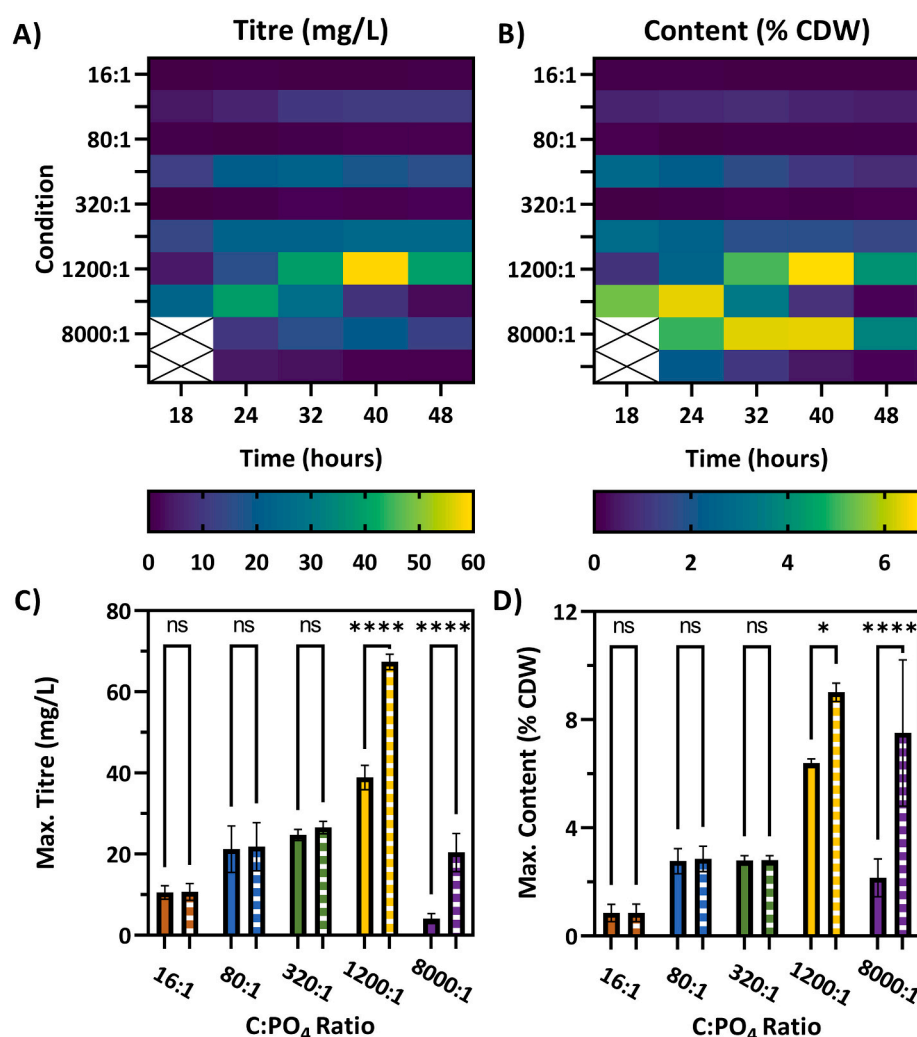


Fig. 4. Heat maps comparing TAG and WE accumulation over for time different C:PO₄ ratios, showing **A)** titre (mg/L) and **B)** content (% CDW). Labelled rows show TAG accumulation for that condition, and row below shows WEs for the same condition, on the same colour gradient. Comparisons of the maximum **C)** titre and **D)** content for just WE accumulation compared to WE and TAG combined. Pairwise comparison between WE and WE + TAG performed by 2-way ANOVA, ns ≥ 0.05 , * = 0.05, ** = 0.01, *** = 0.001, **** = 0.0001.

320:1 titre continued to increase with time. At 1200:1, the first condition under which growth was severely impaired, WE titre and content was initially high, reaching a maximum of 39 ± 3 mg/L with a content of 6.4 ± 0.2 % CDW, then decreased rapidly to near zero. Extreme phosphate limitation demonstrated negative effects on WE accumulation; at 8000:1 poor growth resulted in very low WE production, with a maximum titre of just 4 ± 1 mg/L.

A mixed effects statistical model identified C:PO₄ ratio had significant effects on WE titre, % CDW and conversion efficiency, with $p < 0.0001$ for all. By the same analysis, time had a significant impact on content ($p < 0.001$) and conversion efficiency ($p < 0.01$), but was not a significant factor in titre. This is consistent with all conditions showing higher contents and efficiencies at earlier timepoints, while for titre, 16:1 and 320:1 increased with time while 1200:1 and 8000:1 decreased.

Pairwise comparison between maximum values of C:PO₄ ratios, as shown in Fig. 3D, E and F, showed that titre ($p < 0.01$) and wax content ($p < 0.001$) increased significantly from 16:1 to 80:1, although the difference in conversion efficiency was not significant. At 80:1 and 320:1 production was comparable, but, by all metrics, the greatest and most efficient WE production was achieved at 1200:1. Above this, production decreased significantly due to extreme phosphate starvation.

Under extreme phosphate starvation conditions (1200:1 and 8000:1), significant triacylglycerol (TAG) production and accumulation was also detected. Fig. 4 shows the TAG production relative to the WE production over time, both in titre and content per cell, for all C:PO₄ ratios tested, and the maximum combined lipid production (TAGs+WEs)

compared to just WEs. Up to 320:1, negligible TAGs were detected at all times, while at 2:000:1 a maximum of 59 ± 1 mg/L of TAG was produced after 40 h, higher than the maximum WE production under this condition, and the maximum across all conditions, of 39 ± 3 mg/L, which occurred after 24 h. At 8000:1, the maximum TAG titre of 19 ± 5 mg/L was achieved at 40 h, which accounted for 6 ± 1 % of CDW, almost 5-fold the maximum WE accumulation of 4 ± 1 mg/L at 24 h, accounting for 2.2 ± 0.7 % CDW.

The transition from accumulation of WEs to TAGs at high C:PO₄ ratios is previously unreported in the literature. Work by Salcedo-Vite *et al* has previously shown that ADP1 accumulates different ratios of TAGs: WEs when grown on different carbon sources, though on acetate the authors observed no TAG production (Salcedo-Vite *et al.*, 2019), in agreement with the other conditions tested here.

Cellular responses to phosphate limitation tend to involve gene expression changes to produce proteins for increased extracellular phosphate uptake and to release stored intracellular phosphate. Previous literature has observed the accumulation of lipids, particularly TAGs, due to phosphate starvation in micro-organisms (Wu *et al.*, 2010; Yang *et al.*, 2018a), in agreement with the results observed here. Based on this, TAGs should be considered as a phosphate source, metabolites whose synthesis results in the release of phosphate, and thus synthesis of these molecules increases as a response to phosphate limitation (Gupta and Laxman, 2021). Such molecules do not contain phosphate, but instead have phosphate-containing precursors; TAGs are produced from diacylglycerol phosphates, a class of phospholipids, in a two-step

Table 1

Concentrations of Mg^{2+} , Ca^{2+} and K^+ in the standard media, and with the supplementation of additional mineral ions.

Nutrient	Regular Conc (mM)	+ Conc (mM)
Mg^{2+}	0.95	4.42
Ca^{2+}	0.09	0.21
K^+	15	50

process, the first of which releases phosphate and facilitates conversion of ADP to ATP. Under phosphate rich conditions, glycerol-based phospholipids are used for membranes and cell walls, but under extreme phosphate starvation, phosphate must be released for other essential metabolic uses, including ATP generation. TAG production thus allows phosphate release, whilst maintaining efficient carbon storage.

Whilst explaining the increase in TAG production under phosphate starvation, this does not directly explain the rapid accumulation then depletion of WEs observed at 1200:1 C:PO₄. Upregulation of fatty acid synthesis is a known response to phosphate limitation (Huang et al., 2019; Wang et al., 2018), and, with sufficient nutrient concentrations, in ADP1 this accumulation would naturally lead to WE production. However, fatty acid anabolism requires many equivalents of reducing agents NADH and NADPH, both of which have been observed to be broken down under phosphate depletion (Wang et al., 2018). With severe phosphate starvation, as observed at 8000:1 and in later timepoints at 1200:1, the intracellular concentration of NADH and NADPH is expected to decrease, limiting fatty acid production. It is therefore hypothesised

that accumulated WEs would be degraded under these conditions to produce fatty acids for a plethora of cellular functions, potentially including TAG synthesis to release further phosphate. Such a hypothesis could be examined by feeding carbon-labelled WEs to phosphate-starved ADP1, then testing extracted TAGs for the appropriate labelling. However, such experimentation is beyond the scope of this work.

3.3. Micronutrient limitation

The minimal media recipe employed here (Kennerley, 2022) contained significantly lower concentrations of micronutrients than media reported in other WE accumulation studies in ADP1 (Kannisto et al., 2014; Lehtinen et al., 2018). To test whether this influenced WE production, the concentrations of 3 key micronutrients were increased individually, based on the maximum concentrations used in literature recipes (Kannisto et al., 2014). Mg^{2+} , Ca^{2+} and K^+ ions were chosen specifically due to their known cellular functions, links to lipid production and having the greatest concentration difference between recipes. The exact concentrations of each ion tested are given in Table 1. The effect of culturing ADP1 without a trace elements mix was also explored, since in many reports they are not required for high wax production (Kannisto et al., 2014; Luo et al., 2020). Cultures were grown at C:N and C:PO₄ ratios of 20:1 and 320:1, respectively.

Maximal growth was reduced by approximately 10 % when TEs were omitted (Fig. 1C), but the effect on WE production was minimal (Fig. 5). Conversely, increasing Mg^{2+} and Ca^{2+} concentration, independently, improved maximum growth by around 25 %. An increase in WE

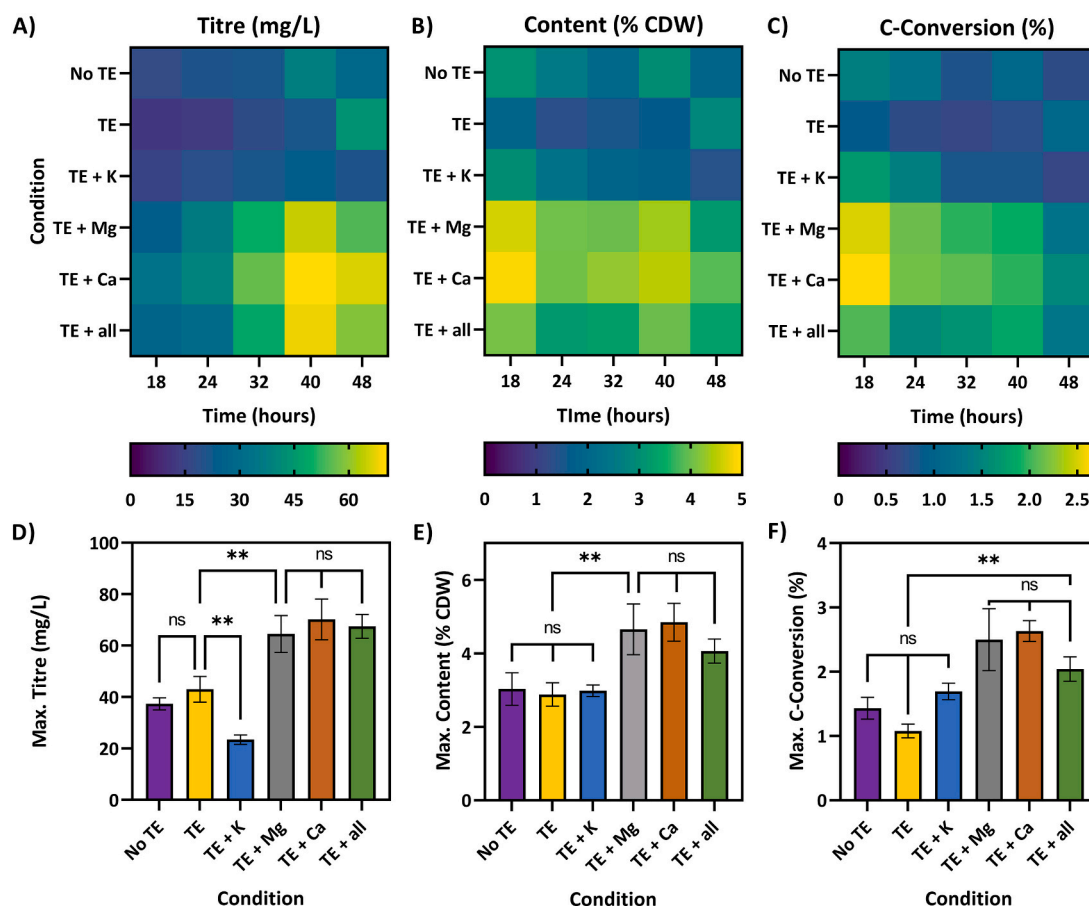


Fig. 5. Heat maps showing A) WE titre (mg/L), B) WE content per biomass (% CDW) and C) Carbon conversion efficiency from acetate to WEs (%), over time under different micronutrient conditions. Data shows means of 3 biological replicates, values from blue (low) to yellow (high). Maximum achieved D) WE titre (mg/L), E) WE content per biomass (% CDW) and F) Carbon conversion efficiency to WEs (%) for each condition. Data shows means and error bars represent standard deviation ($n = 3$). Multiple comparison tests were performed between all conditions, ns ≥ 0.05 , * = 0.05, ** = 0.01. All p -values given in supplementary information. (For interpretation of the references to colour in this figure legend, the reader is referred to the web version of this article.)

production was also observed, from a maximum of 43 ± 5 mg/L in TE media to 65 ± 7 mg/L and 70 ± 8 mg/L in media with TEs plus additional Mg^{2+} and Ca^{2+} respectively. Similar trends were observed in WE content, with increased Ca^{2+} concentration resulting in the greatest WE content per cell of 4.8 ± 0.5 % CDW, compared to 2.9 ± 0.3 % CDW with the standard media with TEs. Conversely, increased K^+ concentration restricted WE production, with a maximum titre of just 23 ± 2 mg/L, despite improving maximum growth by around 10 % compared to TE media. Maximum WE content per cell was 3.0 ± 0.2 % CDW, equal to that of the standard media with TEs, but it occurred earlier in time when growth was lower. The combination of increasing all 3 nutrients was also tested to account for any interaction between their effects. In this case, the behaviour observed was very similar to the addition of either Mg^{2+} or Ca^{2+} individually, with improved growth and maximal WE titre and content of 67 ± 5 mg/L and 4.1 ± 0.3 % CDW respectively.

A mixed effects statistical model identified time, condition and the interaction of the two to be significant ($p < 0.0001$ for all metrics), with overall trends that titre increased with time for most conditions, while content and C-conversion decreased with time. Pairwise comparison between maxima showed no statistical difference between with or without TEs on any metric. Similarly, there was no pairwise difference between any of TE + Mg^{2+} , TE + Ca^{2+} and TE + all, on any metric. However, for all metrics, WE production under each of these three conditions was significantly greater than both with and without TEs ($p < 0.01$). The maximum WE titre achieved TE + K^+ was significantly lower than for TE, but maximum content and conversion were comparable.

The negligible effect of TEs on WE production suggests ADP1 cells may accumulate and store sufficient TEs for multiple generations. Several studies have utilised media without TEs for WE production in ADP1 (Kannisto et al., 2014; Luo et al., 2020), including the highest reported WE titre from the wild type bacteria (Luo et al., 2020), supporting these findings. To observe the true effect of TE limitation, sequential culturing in the absence of TEs may be needed prior to growth and production experiments. However, this was beyond the scope of this study. The growth improvement in the presence of TEs may, however, be beneficial under growth-limiting conditions, such as nutrient limitations.

Increasing the concentration of Ca^{2+} has previously been shown to increase growth rate and maximum OD in other species of *Acinetobacter* (Chen et al., 2019), in agreement with the observed growth behaviour for the TE + Ca^{2+} and TE + all samples. Similarly, both Ca^{2+} and Mg^{2+} deficiency have been shown to limit maximum growth in other bacteria (Vincent, 1962). However, in all cases in which Ca^{2+} , Mg^{2+} or both were increased in concentration, the WE content per cell also increased, indicating an additional effect beyond just growth improvement, and suggesting the benefits to lipid production previously observed in microalgae may translate to bacteria (Huang et al., 2014; Singh et al., 2016). Conversely though, in this work increasing K^+ concentration did not yield equivalent lipid-accumulation benefits as previously reported in other micro-organisms (Janchot et al., 2019).

The benefits of additional Ca^{2+} and Mg^{2+} were similar in magnitude and were not compounding, suggesting the improved growth and lipid production achieved at higher nutrient concentrations originated from a metabolic function which can be fulfilled by either ion. Previously, it was observed that *E. coli* mutants with a higher minimum Mg^{2+} requirement could utilise Ca^{2+} ions as a substitute, and, when Mg^{2+} was replaced by Ca^{2+} , the necessary concentration was much lower (Lusk et al., 1968). Although the same was not observed for WT *E. coli*, in that additional Ca^{2+} did not affect growth regardless of Mg^{2+} concentration, other bacterial species have been shown to benefit from additional, non-specific divalent ions. Specifically, *Rhizobium trifolii* has been demonstrated to require a minimum total divalent ion concentration which was met by either Ca^{2+} or Mg^{2+} , as well as individual minimum concentrations of both, in order to avoid signs of deficiency, including reduced growth (Vincent, 1962).

Table 2

The parameter space of conditions explored in the multifactor C:N and C:PO₄ experiment.

Condition	N Level	P Level	C:N Ratio	C:PO ₄ Ratio	N:P ratio	Number of replicates
1	-1	-1	40:1	450:1	11.25:1	2
2	-1	1	40:1	1350:1	33.75:1	2
3	1	-1	80:1	450:1	5.63:1	2
4	1	1	80:1	1350:1	16.88:1	2
5	$-\sqrt{2}$	0	32:1	900:1	28.13:1	2
6	$\sqrt{2}$	0	88:1	900:1	10.23:1	2
7	0	$-\sqrt{2}$	60:1	264:1	4.39:1	2
8	0	$\sqrt{2}$	60:1	1536:1	25.61:1	2
9	0	0	60:1	900:1	15.00:1	4

Given the results of using additional Mg^{2+} , Ca^{2+} and all 3 ions (Mg^{2+} , Ca^{2+} and K^+) were comparable across all metrics, the optimal nutrient was chosen by efficiency, as a combination of quantity and cost. To achieve these effects, an additional 0.9 g/L of $MgSO_4 \cdot 7H_2O$ was used, compared to just 18 mg/L of $CaCl_2$. Based on a bulk-cost of approximately \$100/t for both $CaCl_2$ and $MgSO_4 \cdot 7H_2O$ (typical price on Alibaba at time of writing), this results in a 50-fold price difference between the required quantities of the two reagents, making additional Ca^{2+} supplementation the obvious choice.

3.4. Multifactor experiment

Based upon the findings of the previous 3 experiments, a multi-factor experiment was designed to explore the WE production landscape within a more targeted range of C:N and C:PO₄ concentrations, with the aim to investigate possible combined effects of N and PO₄ limitation on WE production. A 2-factor, central composite designed experiment was constructed, with parameters for each variable as given in Table 2.

A C:N range of 40:1–80:1 was chosen, which encompassed the maxima in both WE content and titre. For C:PO₄, 1200:1 was shown to yield the greatest WE titre and content, but this occurred at early time points and subsequently depleted over time. Conversely, at 320:1, WEs accumulated over time, suggesting the optimal C:PO₄ ratio for WE accumulation lies between these two ratios. Furthermore, WE accumulation behaviour at 320:1 was more similar, and therefore perhaps would be more complimentary, to that due to N limitation. Since N limitation also showed a greater relative and absolute effect on WE production, a C:PO₄ range of 450:1–1350:1 was selected, with an aim of maximising WE production and the possible interaction between N and PO₄ limitation. TEs were included in the media based on their benefit to growth and the maximum concentration of Ca^{2+} was also included for the growth and WE production benefits observed.

3.4.1. Wax ester production

Fig. 6A and B show surface response plots for WE titre and content, while Table 3 contains statistical information about the fits and significances calculated. Local maxima in titre were achieved at the minimum and maximum N:PO₄ ratios, which occur at the maximum level of one nutrient and the minimum level of the other, while, where both nutrients were present at the same level (either 40:1, 450:1 or 80:1, 1350:1), titre decreased to a local minimum. Across the whole range, a minimum and maximum titre of 110 ± 10 mg/L and 150 ± 30 mg/L were observed, respectively. WE content varied from 7.8 ± 0.8 % to 17 ± 3 %, with higher C:N ratios consistently resulting in higher WE content over the range analysed. In both titre and content, the absolute maximum was achieved at the higher C:N ratio (80:1) and lower C:PO₄ ratio (450:1), which corresponds to the lowest N:PO₄ ratio.

Student's *t*-test performed on the coded coefficients determined that the interaction coefficient of C:N and C:PO₄, equivalent to N:PO₄, and the C:N squared term were significant for fitting the contour plots of both the WE titre and content ($p < 0.01$ for all; see Table 3), and that the

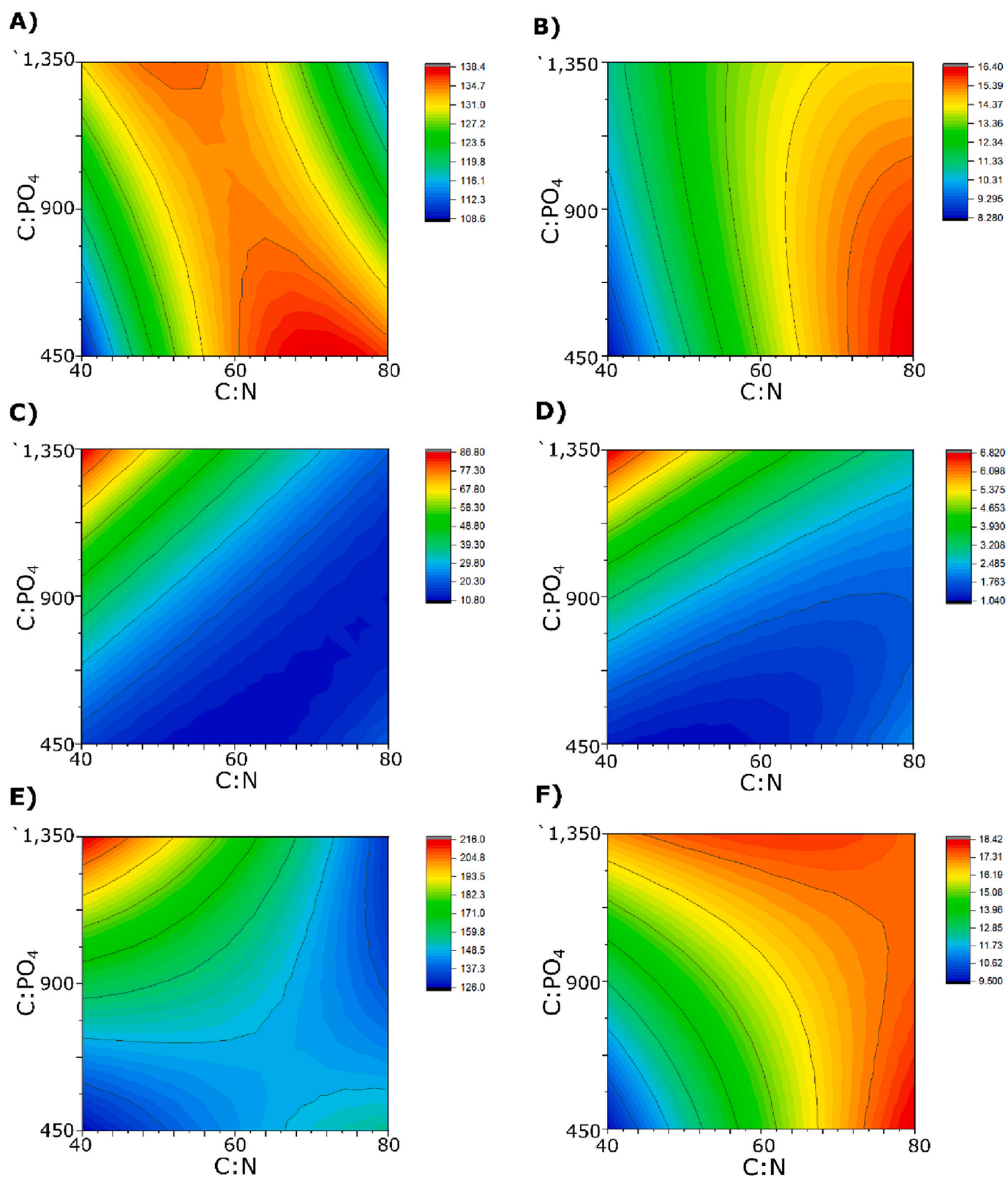


Fig. 6. Contour plots showing the maximum titre and content of the different lipids detected when C:N and C:PO₄ were co-varied. **A)** titre and **B)** content per cell of WEs; maximum **C)** titre and **D)** content per cell of TAGs and the maximum **E)** titre and **F)** content per cell of combined lipids (WEs + TAGs).

Table 3

Key statistical values determined for each linear factor, quadratic factor and the interaction factor from full quadratic models fitted to the multivariable experiment data for WE production. Lower and Upper Confidence Interval (LCI and UCI) are 95 %.

	Coefficient value [LCI, UCI]	p value (t-statistic)	DF (x,y)	F Value	p value (F-statistic)
Titre					
C:N	2.10 [-6.49, 10.7]	0.519	(1,14)	0.27	0.608
C:PO ₄	-0.46 [-9.05, 8.12]	0.886	(1,14)	0.01	0.910
C:N x C:N	-11.9 [-23.2, -0.52]	0.003 **	(1,14)	6.02	0.028 *
C:PO ₄ x C:PO ₄	-0.33 [-11.7, 11.0]	0.919	(1,14)	0.00	0.952
C:N x C:PO ₄	-11.7 [-23.8, 0.45]	0.003 **	(1,14)	4.26	0.058
Content					
C:N	2.92 [2.22, 3.61]	6.82×10^{-7} ****	(1,14)	80.5	3.53×10^{-7} ****
C:PO ₄	0.19 [-0.51, 0.89]	0.525	(1,14)	0.34	0.568
C:N x C:N	-1.07 [-1.99, -0.15]	0.004 **	(1,14)	5.65	0.032 *
C:PO ₄ x C:PO ₄	-0.34 [-1.26, 0.58]	0.263	(1,14)	0.63	0.441
C:N x C:PO ₄	-1.13 [-2.11, -0.15]	0.002 **	(1,14)	6.09	0.027 *

Asterisks indicate significance at levels as follows: * = 0.05, ** = 0.01, *** = 0.001 and **** = 0.0001.

C:N ratio coefficient was highly significant in determining WE content ($p < 0.0001$). This interaction can clearly be seen in the contour plots (Fig. 6A and B). For titre, the plot has a distinct saddle shape; when one nutrient is fixed at the lower level, increasing the ratio of the other nutrient increased WE titre, yet when either nutrient was fixed at the higher level, increasing the other nutrient decreased WE titre. For WE content, at all C:PO₄ ratios, a higher C:N ratio resulted in higher WE content per cell. However, at C:PO₄ of 450:1 this effect was much more pronounced than at 1350:1. This result led to behaviour whereby at C:N of 40:1, increasing C:PO₄ ratio increased WE content per cell, yet at C:N 60:1 there was a negligible effect and by C:N 80:1 this was reversed and a lower C:PO₄ ratio (more PO₄) was favourable for higher WE content. Statistical analysis of the data by ANOVA confirmed the effect of C:N ratio on content was highly significant ($p = 3.53 \times 10^{-7}$). C:N squared was also significant on both titre and content, and the interaction of C:N x C:PO₄ significantly affected content ($p < 0.05$ for all).

The observed significance of C:N ratio on WE content per cell is in agreement with previous studies for other lipid accumulating species (Castro et al., 2018), though this is the first time such a comprehensive study has been performed for ADP1. Similarly, no study has previously explored the relationship between C:N and C:PO₄ ratio in bacteria. This relationship was found to be significant on WE content over the ranges sampled here, and a significant factor in the regression model of both content and titre.

The maximum WE titre and content recorded in this experiment were 150 ± 30 mg/L and 17 ± 3 % CDW respectively and were achieved simultaneously. These are just short of the literature maxima from

acetate of 184 mg/L and 19 % CDW (Santala et al., 2018), achieved by a genetically engineered strain of ADP1. In that instance, an additional 5 g/L of arabinose inducer was required, which has previously been highlighted as inefficient and economically infeasible (Martin et al., 2021). This highlights the significance and potential of nutrient limitation as a factor in bacterial lipid production.

3.4.2. Triacylglycerol (TAG) production

Since significant TAG production was detected in the C:PO₄ ratio experiment, neutral lipid extracts from the multivariable experiment were also analysed for the presence of TAGs. TAG production was observed under all conditions tested. The trend of increasing TAG with increasing C:PO₄ ratio was strong at C:N 40:1, although by C:N 80:1 the change was negligible (Fig. 6C and D).

The optimal condition for TAG production was found to be at the maximum N:PO₄ ratio (the minimum C:N of 40:1 and maximum C:PO₄ of 1350:1), where the titre was 91.6 ± 0.6 mg/L and content 7.29 ± 0.09 % CDW. Under this same condition the WE titre was 120 ± 10 mg/L and content was 10 ± 1 % CDW, resulting in a WE:TAG mass ratio of 1.3:1. The minimum TAG accumulation also occurred at C:N 40:1, but with C:PO₄ of 450:1, under which the TAG titre was 15.0 ± 0.3 mg/L and content was 1.09 ± 0.03 %. This coincided with the minimum WE accumulation with a titre of 110 ± 10 mg/L and content of 7.8 ± 0.8 % CDW, with a WE:TAG mass ratio of 7:1. When analysed statistically (see Table 4), all factors were highly significant on titre ($p < 0.001$ for both statistics), with the exception of C:N squared, the significance of which was found by ANOVA to be much smaller ($p < 0.05$). The effects on

Table 4

Key statistical values determined for each linear factor, quadratic factor and the interaction factor from full quadratic models fitted to the multivariable experiment data for TAG production. Lower and Upper Confidence Interval (LCI and UCI) are 95 %.

	Coefficient value [LCI, UCI]	p value (t-statistic)	DF (x,y)	F Value	p value (F-statistic)
Titre					
C:N	-15.8 [-18.9, -12.7]	1.22×10^{-8} ****	(1,14)	119	3.23×10^{-8} ****
C:PO ₄	17.5 [14.4, 20.6]	4.15×10^{-9} ****	(1,14)	146	8.72×10^{-9} ****
C:N x C:N	7.78 [3.66, 11.9]	1.48×10^{-5} ****	(1,14)	6.20	0.026 *
C:PO ₄ x C:PO ₄	8.08 [3.96, 12.2]	1.05×10^{-5} ****	(1,14)	17.7	8.83×10^{-4} ***
C:N x C:PO ₄	-17.3 [-21.7, -12.9]	4.86×10^{-9} ****	(1,14)	70.6	7.68×10^{-7} ***
Content					
C:N	-0.75 [-1.03, -0.46]	1.56×10^{-5} ****	(1,14)	30.6	7.37×10^{-5} ****
C:PO ₄	1.58 [1.29, 1.87]	8.30×10^{-9} ****	(1,14)	138	1.24×10^{-8} ****
C:N x C:N	0.51 [0.13, 0.89]	4.11×10^{-4} ***	(1,14)	1.46	0.248
C:PO ₄ x C:PO ₄	0.74 [0.35, 1.12]	1.74×10^{-5} ****	(1,14)	17.1	0.001 **
C:N x C:PO ₄	-1.23 [-1.64, -0.83]	1.10×10^{-7} ****	(1,14)	42.0	1.45×10^{-5} ***

Asterisks indicate significance at levels as follows: * = 0.05, ** = 0.01, *** = 0.001 and **** = 0.0001.

content were similar, with all factors significant ($p < 0.01$) except C:N squared ($p = 0.248$).

At C:PO₄ of 320:1 in the single-variable experiment, with a C:N of 10:1, the WE:TAG mass ratio was 14:1 at maximum lipid accumulation, and including TAGs did not significantly alter the maximum achieved titre or content compared to WEs alone (see Fig. 4C and D). In this experiment, a C:PO₄ ratio of 450:1 resulted in WE:TAG mass ratios of 7:1 and 9:1 at C:N of 40:1 and 80:1, respectively, representing a 2-fold change in the relative abundances of the different lipid classes. WE and combined lipid accumulation increased approximately 4 and 6-fold at the two C:N ratios, respectively. This further supports the evidence that phosphate starvation results in a greater TAG production and TAGs representing a greater proportion of the cellular storage lipids.

Crucially, as no TAGs were detected in the C:N single-variable experiment, despite nitrogen starvation and lipid accumulation, the conclusion that TAG production is induced by phosphate starvation is still supported, and the increasing TAG accumulation with increasing phosphate limitation at C:N 40:1 strengthens this conclusion. The interaction of the C:N and C:PO₄ is highlighted by the fact that both the minimum and maximum TAG accumulation were achieved at 40:1 C:N, yet at 80:1 C:N the maximum TAG titre was minimal and did not change significantly with C:PO₄ ratio.

3.4.3. Combined lipid production

Conditions under which maximum combined lipid production was achieved were also modeled (Fig. 6E and F). For titre, the distribution of minima and maxima remained largely the same as that for WEs, which made up between 56 % and 89 % of lipids for all samples. However, when both WEs and TAGs were considered, the overall maximum moved from the minimum N:PO₄ ratio to the maximum N:PO₄ ratio, with a maximum combined lipids of 210 ± 10 mg/L.

For combined lipid content, the plot resembled that for WEs, with the minimum and maximum still occurring at the same points, and a maximum content of 19 ± 3 % CDW. However, the effect of C:PO₄ ratio on content was more pronounced at low compared to high C:N ratios, while for the WE plot the effect was more prominent at high C:N ratios. The lowest N:PO₄ ratio was preserved as the optimal WE accumulation condition, resulting in both the greatest quantity and purity of WEs, due to the highest WE:TAG mass ratio of 9:1. Statistically, combined lipid titre and content were not significantly affected by C:N squared or C:PO₄ squared, but were affected by C:N, C:PO₄ and N:PO₄ ratio, as determined by both ANOVA and *t*-test of the coefficient effect on the model ($p < 0.01$ for all, see Table 5).

Table 5

Key statistical values determined for each linear factor, quadratic factor and the interaction factor from full quadratic models fitted to the multivariable experiment data for combined lipid production (WEs + TAGs). Lower and Upper Confidence Interval (LCI and UCI) are 95 %.

	Coefficient value [LCI, UCI]	<i>p</i> value (<i>t</i> -statistic)	DF (x,y)	F Value	<i>p</i> value (F-statistic)
Titre					
C:N	-13.9 [-22.2, -5.68]	2.47×10^{-5} ****	(1,14)	13.1	1.43×10^{-5} ****
C:PO ₄	16.45 [8.20, 24.7]	5.35×10^{-4} ***	(1,14)	18.3	4.90×10^{-4} ***
C:N x C:N	-3.50 [-14.4, 7.42]	0.068	(1,14)	2.02	0.069
C:PO ₄ x C:PO ₄	7.08 [-3.83, 18.0]	0.270	(1,14)	1.94	0.426
C:N x C:PO ₄	-28.4 [-40.0, -16.7]	5.22×10^{-5} ****	(1,14)	27.2	8.56×10^{-4} ***
Content					
C:N	2.32 [1.55, 3.08]	0.002 **	(1,14)	42.1	0.003 **
C:PO ₄	1.61 [0.85, 2.38]	5.78×10^{-4} ***	(1,14)	20.3	7.68×10^{-4} ***
C:N x C:N	-0.68 [-1.69, 0.34]	0.332	(1,14)	3.89	0.177
C:PO ₄ x C:PO ₄	0.39 [-0.63, 1.40]	0.064	(1,14)	0.67	0.186
C:N x C:PO ₄	-2.13 [-3.21, -1.05]	5.00×10^{-6} ****	(1,14)	17.8	1.32×10^{-4} ***

Asterisks indicate significance at levels as follows: * = 0.05, ** = 0.01, *** = 0.001 and **** = 0.0001.

4. Conclusion

In this study the significance of nutrient limitation on controlling and improving WE accumulation in *A. baylyi* ADP1 was investigated. By controlling carbon: nitrogen ratio, a 16-fold increase in WE titre and a 15-fold increase in WE content per cell were achieved. Furthermore, more extreme nitrogen starvation did not always result in greater WE accumulation, highlighting the importance of such investigations in optimising future production processes.

For the first time, the effect of carbon: phosphate ratio on WE accumulation was demonstrated, with a maximum 4-fold increase in titre and 7-fold increase in content. The preferred storage lipid class changed from WEs to TAGs under extreme starvation, a previously unreported phenomenon. Divalent cations Mg²⁺ and Ca²⁺ were also shown to contribute to lipid production, with a > 50 % increase in both WE titre and content when these were supplemented at higher concentrations.

By a multivariable analysis within an optimal subset of carbon: nitrogen and carbon: phosphate ratios, it was demonstrated that, as well as nitrogen having a significant effect on WE content, the interaction of the two variables was also significant in WE accumulation. Nitrogen: phosphate ratio was also observed to affect TAG accumulation, which occurred at more moderate carbon: phosphate ratios under lipid accumulating conditions (moderate-high C:N ratios). These findings highlight the importance of condition exploration in attempts to optimise the production of WEs and other biochemicals, and guide future decisions on bioreactor conditions and optimisation.

CRediT authorship contribution statement

Laura Martin: Conceptualisation, Methodology, Investigation, Validation, Formal Analysis, Writing – Original Draft and Review/Editing, Visualisation. **Wei Huang:** Resources, Supervision and Funding Acquisition. **Ian Thompson:** Resources, Writing – Review/Editing, Supervision and Funding Acquisition.

Declaration of competing interest

The authors declare the following financial interests/personal relationships which may be considered as potential competing interests: Laura K Martin reports financial support was provided by Engineering and Physical Sciences Research Council.

Data availability

Data will be made available on request.

Acknowledgements

This work was supported by the EPSRC, UKRI (EP/N509711/1).

Appendix A. Supplementary data

Supplementary data to this article can be found online at <https://doi.org/10.1016/j.biteb.2023.101423>.

References

- Bart, J.C.J., Gucciardi, E., Cavallaro, S., 2013. In: Renewable Feedstocks for Lubricant Production, pp. 121–248.
- Bauchop, T., Elsdon, S.R., 1960. The growth of micro-organisms in relation to their energy supply. *Microbiology* 23 (3), 457–469.
- Castro, A.R., Silva, P.T.S., Castro, P.J.G., Alves, E., Domingues, M.R.M., Pereira, M.A., 2018. Tuning culturing conditions towards the production of neutral lipids from lubricant-based wastewater in open mixed bacterial communities. *Water Res.* 144, 532–542.
- Chen, Y., Shao, T., Fang, S., Pan, P., Jiang, J., Cheng, T., Wan, H., Yu, D., 2019. Effect of calcium on the interaction of *Acinetobacter baumannii* with human respiratory epithelial cells. *BMC Microbiol.* 19 (1).
- Cronan, J.E., Thomas, J., 2009. Chapter 17: bacterial fatty acid synthesis and its relationships with polyketide synthetic pathways. In: *Complex Enzymes in Microbial Natural Product Biosynthesis, Part B: Polyketides, Aminocoumarins and Carbohydrates*, pp. 395–433.
- Deshpande, S., Durdagi, S., Noskov, S.Y., 2013. In: *Potassium in Biological Systems*. Springer, New York, pp. 1799–1804.
- Dominguez, D.C., 2004. Calcium signalling in bacteria. *Mol. Microbiol.* 54 (2), 291–297.
- Gupta, R., Laxman, S., 2021. Cycles, sources, and sinks: conceptualizing how phosphate balance modulates carbon flux using yeast metabolic networks. *eLife* 10.
- Huang, B., Marchand, J., Blanckaert, V., Lukomska, E., Ulmann, L., Wielgosz-Collin, G., Rabesaotra, V., Moreau, B., Bougaran, G., Mimouni, V., Morant-Manceau, A., 2019. Nitrogen and phosphorus limitations induce carbon partitioning and membrane lipid remodelling in the marine diatom *Phaeodactylum tricornutum*. *Eur. J. Phycol.* 54 (3), 342–358.
- Huang, L., Xu, J., Li, T., Wang, L., Deng, T., Yu, X., 2014. Effects of additional Mg²⁺ on the growth, lipid production, and fatty acid composition of *Monoraphidium* sp. FYX-10 under different culture conditions. *Ann. Microbiol.* 64 (3), 1247–1256.
- Huang, X., Luo, H., Mu, T., Shen, Y., Yuan, M., Liu, J., 2018. Enhancement of lipid accumulation by oleaginous yeast through phosphorus limitation under high content of ammonia. *Bioresour. Technol.* 262, 9–14.
- Ikarán, Z., Suárez-Alvarez, S., Urreta, I., Castañón, S., 2015. The effect of nitrogen limitation on the physiology and metabolism of *Chlorella vulgaris* var L3. *Algal Res.* 10, 134–144.
- Ishige, T., Tani, A., Sakai, Y., Kato, N., 2003. Wax ester production by bacteria. *Curr. Opin. Microbiol.* 6 (3), 244–250.
- Janchot, K., Raulytanapanit, M., Honda, M., Hibino, T., Sirisattha, S., Praneenarat, T., Kageyama, H., Waditee-Sirisattha, R., 2019. Effects of potassium chloride-induced stress on the carotenoids canthaxanthin, astaxanthin, and lipid accumulations in the green chlorococcal microalga strain TISTR 9500. *J. Eukaryot. Microbiol.* 66 (5), 778–787.
- Kannisto, M., Aho, T., Karp, M., Santala, V., 2014. Metabolic engineering of *Acinetobacter baylyi* ADP1 for improved growth on gluconate and glucose. *Appl. Environ. Microbiol.* 80 (22), 7021–7027.
- Kennerley, J., 2022. An Evolving Synthetic Biology Platform for Alkane Production. Department of Engineering Science, Vol. Doctor of Philosophy, University of Oxford, Oxford.
- Kong, F., Ren, H.Y., Pavlostathis, S.G., Nan, J., Ren, N.Q., Wang, A., 2020. Overview of value-added products bioelectrosynthesized from waste materials in microbial electrosynthesis systems. *Renew. Sust. Energ. Rev.* 125, 109816.
- Lehtinen, T., Efimova, E., Santala, S., Santala, V., 2018. Improved fatty aldehyde and wax ester production by overexpression of fatty acyl-CoA reductases. *Microb. Cell Factories* 17 (1), 1–10.
- Lehtinen, T., Efimova, E., Tremblay, P.L., Santala, S., Zhang, T., Santala, V., 2017. Production of long chain alkyl esters from carbon dioxide and electricity by a two-stage bacterial process. *Bioresour. Technol.* 243 (October), 30–36.
- Lennen, R.M., Pfleger, B.F., 2013. Microbial production of fatty acid-derived fuels and chemicals. *Curr. Opin. Biotechnol.* 24 (6), 1044–1053.
- Liu, N., Qiao, K., Stephanopoulos, G., 2016. (13)C metabolic flux analysis of acetate conversion to lipids by *Yarrowia lipolytica*. *Metab. Eng.* 38, 86–97.
- Luo, J., Efimova, E., Losoi, P., Santala, V., Santala, S., 2020. Wax ester production in nitrogen-rich conditions by metabolically engineered *Acinetobacter baylyi* ADP1. *Metab. Eng. Commun.* 10, e00128.
- Lusk, J.E., Williams, R.J.P., Kennedy, E.P., 1968. Magnesium and the growth of *Escherichia coli*. *J. Biol. Chem.* 243 (10), 2618–2624.
- Manilla-Pérez, E., Lange, A.B., Luftmann, H., Robenek, H., Steinbüchel, A., 2011. Neutral lipid production in *Alcanivorax borkumensis* SK2 and other marine hydrocarbonoclastic bacteria. *Eur. J. Lipid Sci. Technol.* 113 (1), 8–17.
- Martin, L.K., Huang, W.E., Thompson, I.P., 2021. Bacterial wax synthesis. *Biotechnol. Adv.* 46, 107680.
- Mohr, A., Raman, S., 2013. Lessons from first generation biofuels and implications for the sustainability appraisal of second generation biofuels. *Energy Policy* 63 (100), 114–122.
- Nieva-Echevarría, B., Goicoechea, E., Manzanos, M.J., Guillén, M.D., 2014. A method based on 1H NMR spectral data useful to evaluate the hydrolysis level in complex lipid mixtures. *Food Res. Int.* 66, 379–387.
- Patel, A., Mahboubi, A., Horvath, I.S., Taherzadeh, M.J., Rova, U., Christakopoulos, P., Matsakas, L., 2021. Volatile fatty acids (VFAs) generated by anaerobic digestion serve as feedstock for freshwater and marine oleaginous microorganisms to produce biodiesel and added-value compounds. *Front. Microbiol.* 12, 614612.
- Peterson, C.N., Mandel, M.J., Silhavy, T.J., 2005. *Escherichia coli* starvation diets: essential nutrients weigh in distinctly. *J. Bacteriol.* 187 (22), 7549–7553.
- Pomraning, K.R., Kim, Y.-M., Nicora, C.D., Chu, R.K., Bredeweg, E.L., Purvine, S.O., Hu, D., Metz, T.O., Baker, S.E., 2016. Multi-omics analysis reveals regulators of the response to nitrogen limitation in *Yarrowia lipolytica*. *BMC Genomics* 17 (1).
- Poontawe, Limtong, 2020. Feeding strategies of two-stage fed-batch cultivation processes for microbial lipid production from sugarcane top hydrolysate and crude glycerol by the oleaginous red yeast *Rhodospiridiobolus fluvialis*. *Microorganisms* 8 (2), 151.
- Rottig, A., Hauschild, P., Madkour, M.H., Al-Ansari, A.M., Almakishah, N.H., Steinbüchel, A., 2016. Analysis and optimization of triacylglycerol synthesis in novel oleaginous *Rhodococcus* and *Streptomyces* strains isolated from desert soil. *J. Biotechnol.* 225, 48–56.
- Round, J.W., Rocco, R., Eltis, L.D., 2019. A biocatalyst for sustainable wax ester production: re-wiring lipid accumulation in *Rhodococcus* to yield high-value oleochemicals. *Green Chem.* 21 (23), 6468–6482.
- Salcedo-Vite, K., Sigala, J.C., Segura, D., Gosset, G., Martinez, A., 2019. *Acinetobacter baylyi* ADP1 growth performance and lipid accumulation on different carbon sources. *Appl. Microb. Cell Physiol.* 103, 6217–6229.
- Santala, S., Efimova, E., Karp, M., Santala, V., 2011a. Real-time monitoring of intracellular wax ester metabolism. *Microb. Cell Factories* 10, 1–8.
- Santala, S., Efimova, E., Kivinen, V., Larjo, A., Aho, T., Karp, M., Santala, V., 2011b. Improved triacylglycerol production in *Acinetobacter baylyi* ADP1 by metabolic engineering. *Microb. Cell Factories* 10, 1–10.
- Santala, S., Efimova, E., Santala, V., 2018. Dynamic decoupling of biomass and wax ester biosynthesis in *Acinetobacter baylyi* by an autonomously regulated switch. *Metab. Eng. Commun.* 7.
- Santala, S., Santala, V., 2021. *Acinetobacter baylyi* ADP1—naturally competent for synthetic biology. *Essays Biochem.* 65 (2), 309–318.
- Santala, S., Santala, V., Liu, N., Stephanopoulos, G., 2021. Partitioning metabolism between growth and product synthesis for coordinated production of wax esters in *Acinetobacter baylyi* ADP1. *Biotechnol. Bioeng.* 118 (6), 2283–2292.
- Shrestha, N., Dandinet, K.K., Schneegurt, M.A., 2020. Effects of nitrogen and phosphorus limitation on lipid accumulation by *Chlorella kessleri* str. UTEX 263 grown in darkness. *J. Appl. Phycol.* 32 (5), 2795–2805.
- Singh, D., Barrow, C.J., Puri, M., Tuli, D.K., Mathur, A.S., 2016. Combination of calcium and magnesium ions prevents substrate inhibition and promotes biomass and lipid production in *Thraustochytrids* under higher glycerol concentration. *Algal Res.* 15, 202–209.
- Vincent, J.M., 1962. Influence of calcium and magnesium on the growth of *Rhizobium*. *J. Gen. Microbiol.* 28 (4), 653–663.
- Walker, G.M., 1994. The roles of magnesium in biotechnology. *Crit. Rev. Biotechnol.* 14 (4), 311–354.
- Wang, X., Fosse, H.K., Li, K., Chauton, M.S., Vadstein, O., Reitan, K.I., 2019. Influence of nitrogen limitation on lipid accumulation and EPA and DHA content in four marine microalgae for possible use in aquafeed. *Front. Mar. Sci.* 6.
- Wang, Y., Zhang, S., Zhu, Z., Shen, H., Lin, X., Jin, X., Jiao, X., Zhao, Z.K., 2018. Systems analysis of phosphate-limitation-induced lipid accumulation by the oleaginous yeast *Rhodospiridium toruloides*. *Biotechnol. Biofuels* 11 (1).
- Wierzchowska, K., Zieniuk, B., Nowak, D., Fabiszewska, A., 2021. Phosphorus and nitrogen limitation as a part of the strategy to stimulate microbial lipid biosynthesis. *Appl. Sci.* 11 (24).
- Wu, S., Hu, C., Jin, G., Zhao, X., Zhao, Z.K., 2010. Phosphate-limitation mediated lipid production by *Rhodospiridium toruloides*. *Bioresour. Technol.* 101 (15), 6124–6129.
- Yang, F., Xiang, W., Li, T., Long, L., 2018a. Transcriptome analysis for phosphorus starvation-induced lipid accumulation in *Scenedesmus* sp. *Sci. Rep.* 8 (1).
- Yang, L., Chen, J., Qin, S., Zeng, M., Jiang, Y., Hu, L., Xiao, P., Hao, W., Hu, Z., Lei, A., Wang, J., 2018b. Growth and lipid accumulation by different nutrients in the microalga *Chlamydomonas reinhardtii*. *Biotechnol. Biofuels* 11 (1).
- Zhang, H., Wu, C., Wu, Q., Dai, J., Song, Y., 2016. Metabolic flux analysis of lipid biosynthesis in the yeast *Yarrowia lipolytica* using 13C-labeled glucose and gas chromatography-mass spectrometry. *PLOS ONE* 11 (7), e0159187.